Ecological Indicators 189 (2026) 115160

Contents lists available at ScienceDirect

Ecological Indicators

journal homepage: www.elsevier.com/locate/ecolind

Mangrove expansion in the Mekong Delta continues despite sea-level rise

Tianliang Wu [a,b,1], Aoyang He [a,1], Zhijun Dai [a,c,*], Xuefei Mei [a], Jaap H. Nienhuis [d], Cong Mai Van [e], Nguyen An Binh [f], Sergio Fagherazzi [g]

[a] State Key Laboratory of Estuarine and Coastal Research, East China Normal University, Shanghai 200062, China
[b] Guangxi Academy of Oceanography, Nanning 530022, China
[c] Guangxi Key Laboratory of Marine Environment Change and Disaster in the Beibu Gulf, Beibu Gulf University, Qinzhou 535011, China
[d] Department of Physical Geography, Faculty of Geosciences, Utrecht University, Utrecht, the Netherlands
[e] Faculty of Civil Engineering, Thuyloi University, Hanoi, Viet Nam
[f] Department of Geography and Remote Sensing, Institute of Life Sciences, Vietnam Academy of Science and Technology, Ho Chi Minh City, Viet Nam
[g] Department of Earth and Environment, Boston University, Boston, USA

ARTICLE INFO

Keywords:
Mangrove expansion
Sea-level rise
Sediment-hydrodynamics
Mangrove resilience
Mekong Delta

ABSTRACT

Global deltaic mangroves are threatened by accelerated sea-level rise. However, the extent to which accelerated sea-level rise drives landward mangrove migration remains difficult to verify in modern deltas, where concurrent seaward expansion is often driven by sediment delivery. Part of the complication is that interplay of anthropogenic activities and sediment-hydrodynamics in deltas obscures the mangrove response to sea-level rise. Here we analyze the dynamics of the Mekong Delta mangrove shorelines over 496 km through 1992–2024. We find that, despite high rates of relative sea-level rise (RSLR), there was a net mangrove gain of approximately 46300 ha, with three-quarters occurring landward and one-quarter seaward. The observed landward migration was statistically associated with RSLR and occurred where accommodation space was available, while seaward expansion was linked to river sediment supply and modulated by local hydrodynamic processes. Disparities in landward migration between estuarine and coastal regions underscore challenges to mangrove resilience, reflecting how the mangrove response to RSLR is mediated by anthropogenic constraints. This study provides critical insights to inform adaptive management of mangroves under rising sea levels.

1. Introduction

Approximately 41% of global mangroves are located in tropical and subtropical deltas (Worthington et al., 2020), where they mitigate wave energy, sustain marine habitats, and provide critical carbon storage (Donato et al., 2011; Temmerman et al., 2013). However, these mangrove ecosystems face compounding threats from climate change and human interventions. Global fluvial sediment loads have declined by nearly 49% due to extensive dam construction (Dethier et al., 2022), severely altering the sediment budgets of major river deltas (Leuven et al., 2019). Meanwhile, relative sea-level rise (RSLR) threatens to submerge mangrove forests when local surface accretion fails to keep pace with rising water levels (Lovelock et al., 2015; Spencer et al., 2016).

Despite these global pressures, mangrove survival fundamentally depends on their spatial adaptability through seaward progradation and landward migration. This dual dynamic is primarily governed by a delicate balance among RSLR, sediment supply, and hydrodynamic processes (Rogers et al., 2019; Schuerch et al., 2018; Woodroffe et al., 2016). As RSLR increases the vertical and lateral accommodation space for mangroves, the role of sediment becomes critical. Sufficient fluvial sediment supply that outpaces RSLR effectively fills this accommodation space, enabling mangroves to migrate landward (Besselly et al., 2021; Feng et al., 2020). Conversely, sediment deficits combined with intense hydrodynamic forces accelerate shoreline erosion and seaward retreat (Balke et al., 2015; Xie et al., 2020). Successful landward migration requires continuous sediment deposition to elevate the substrate along with coasts free from human infrastructure. When artificial barriers restrict this inland pathway, mangroves experience coastal squeeze, leading to potential habitat loss (Borchert et al., 2018; Enwright et al., 2016). Therefore, evaluating mangrove sustainability requires assessing both seaward and landward changes simultaneously.

* Corresponding author at: State Key Laboratory of Estuarine and Coastal Research, East China Normal University, Shanghai 200062, China
E-mail address: zjdai@sklec.ecnu.edu.cn (Z. Dai).
[1] The two authors contribute equally to this work.

https://doi.org/10.1016/j.ecolind.2026.115160
Received 30 December 2025; Received in revised form 4 June 2026; Accepted 5 July 2026

The Mekong Delta, the world's third-largest delta (Fig. 1A), provides an ideal environment to investigate these dual migration dynamics. Since the early 1990s, robust conservation policies by the Vietnamese government have curtailed direct mangrove deforestation that was historically driven by shrimp pond expansion (Li et al., 2020; Phan and Stive, 2022). Consequently, dominate drivers of mangrove change have shifted to reduced sediment loads from the Mekong River and accelerating sea-level rise (Fig. 1C–D) (Kondolf et al., 2014; Li et al., 2017). Spanning a 496-km coastline, the delta exhibits marked spatial heterogeneity in sediment supply and coastal infrastructure. Notably, seawalls have primarily been constructed landward of existing mangroves in the estuarine zones, leaving most zones along the coast with few artificial barriers. This uneven development of the shoreline allows us to assess mangrove adaptation to RSLR, contrasting constrained coastal squeeze against unhindered landward migration.

In this study, we present a comprehensive assessment of mangrove spatial dynamics in the Mekong Delta spanning over thirty years. Leveraging 30-m Landsat imagery and a Random Forest (RF) machine learning classifier, we reconstruct the annual mangrove distribution across different zones from 1992 to 2024, identifying decadal-scale trends of mangrove expansion and retreat. Furthermore, we integrate fluvial sediment loads, RSLR, and hydrodynamic factors to examine the influence of these environmental variables on mangrove landward and seaward migration.

2. Materials and methods

2.1. Data acquisition and pre-processing

Landsat Surface Reflectance products were used as the primary remote-sensing data source for mapping mangrove dynamics in the Mekong Delta from 1992 to 2024. The Landsat archive provides the only continuous, systematic, and spatially consistent satellite record suitable for reconstructing multi-decadal mangrove changes since the early 1990s. Landsat 5 TM, Landsat 7 ETM+, Landsat 8 OLI, and Landsat 9 OLI-2 Surface Reflectance images with a spatial resolution of 30 m were accessed and processed using the Google Earth Engine platform. A total of 1617 Landsat scenes covering the study area were used for annual mangrove mapping from 1992 to 2024 (Fig. S1A).

Clouds, cloud shadows, and other low-quality observations were removed using the quality assessment bands provided with the Landsat Surface Reflectance products. To reduce the influence of seasonal variability, residual cloud contamination, short-term inundation, and tidal flooding on mangrove classification, annual median composites were generated for each year. The use of annual median composites is particularly suitable for deltaic mangrove environments because single-date images are often affected by tidal stage and may underestimate mangrove extent along the seaward edge. Based on the annual composites, four spectral indices were calculated to improve the separability

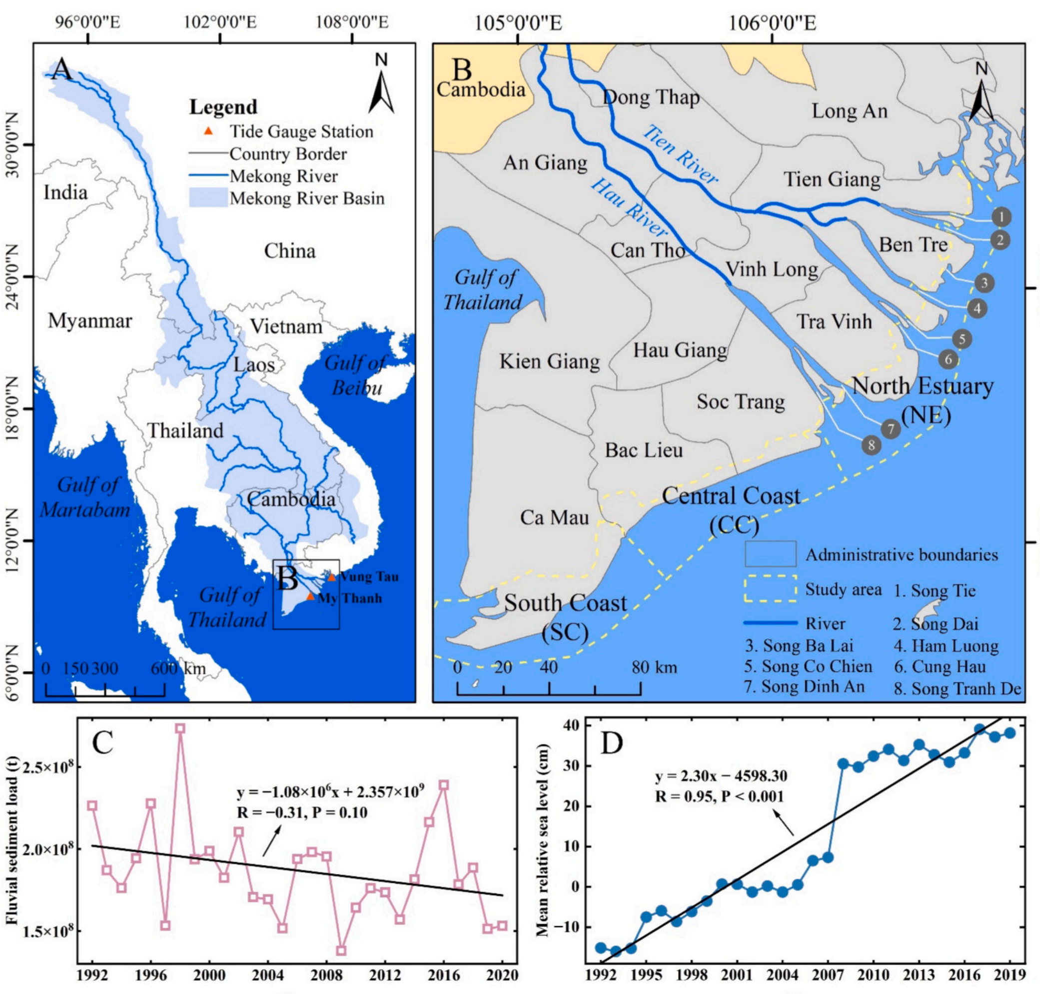

Fig. 1. (A) The Mekong River Basin and the location of the Mekong Delta. The basin boundary was derived from the HydroBASINS dataset (https://www.hydrosheds.org/products/hydrobasins); (B) The three mangrove distribution zones: North Estuary (NE), Central Coast (CC), South Coast (SC); (C) Annual fluvial sediment load of the Mekong River obtained from Dethier et al. (2022); (D) Annual mean relative sea level at the My Thanh tide gauge station, referenced to the Vietnam National Vertical Datum.

among mangroves, water bodies, tidal flats, built-up land, and other vegetation types: the Modified Normalized Difference Water Index, MNDWI; the Normalized Difference Built-up Index, NDBI; the Normalized Difference Vegetation Index, NDVI; and the Mangrove Vegetation Index, MVI (Rouse et al., 1974; Xu, 2006; Zha et al., 2003; Baloloy et al., 2020). These spectral indices (Table S1), together with the original Landsat spectral bands, were used as input variables for mangrove classification.

Hourly tide-level data from the Vung Tau tide-gauge station were obtained from the Sea Level Station Monitoring Facility and were used to identify Landsat scenes acquired under low-tide conditions. These low-tide scenes were not used to generate the annual mangrove maps directly, but were used as independent reference images to evaluate whether the annual median composites could effectively reduce tidal noise along mangrove seaward boundaries. Three optimal low-tide Landsat images, with a mean tide level of approximately 1326 mm, were selected for comparison with annual median composites (Fig. S2; Table S2).

In addition to satellite images, several environmental datasets were compiled to analyze potential drivers of mangrove dynamics. Monthly suspended sediment load data for the Mekong River were obtained from Dethier et al. (2022). Monthly sediment fluxes were aggregated into annual sediment loads for 1992–2020 and used to assess the relationship between river sediment supply and mangrove changes. Relative sea-level data referenced to the Vietnam National Vertical Datum were obtained from the My Thanh tide-gauge station, located near the mangrove seaward edge of the Mekong Delta. Annual mean relative sea level was calculated for 1992–2019 and used to evaluate the potential influence of relative sea-level rise on mangrove migration.

Tropical cyclone records were obtained from the International Best Track Archive for Climate Stewardship. Cyclone tracks affecting the Mekong Delta and adjacent coastal waters from 1992 to 2024 were extracted to calculate annual cyclone frequency and monthly landfall distribution. Offshore current velocities and directions were obtained from the Copernicus Marine Service global physical reanalysis product. Current fields from 1992 to 2024 were used to compare seasonal circulation patterns between the Southwest Monsoon and Northeast Monsoon periods. Offshore wave height and wave direction data were derived from the ECMWF ERA5 reanalysis dataset. Wave direction and significant wave height along the Mekong Delta coast were analyzed to characterize spatial differences in hydrodynamic exposure, particularly for interpreting seaward edge erosion and expansion patterns.

Auxiliary datasets were used for training sample collection and classification validation. These included the Global Mangrove Watch dataset, historical mangrove maps of the Mekong Delta, and high-resolution images from Google Earth. Together, these data sources provided spatial references for mangrove, water, bare flat, and urban or built-up classes.

2.2. Mangrove extraction and accuracy assessment

Mangrove extent was extracted annually from 1992 to 2024 using a RF classifier. RF is an ensemble machine-learning algorithm that integrates multiple decision trees and produces final classifications through majority voting. It is suitable for high-dimensional remote-sensing data and is relatively robust against overfitting and noise (Poortinga et al., 2020). Previous studies have demonstrated its effectiveness in mangrove mapping, including in tidally influenced and frequently flooded coastal environments (Jia et al., 2023; Zablan et al., 2023).

For each annual Landsat median composite, the original spectral bands and four spectral indices, namely MNDWI, NDBI, NDVI, and MVI, were used as input features. Four land-cover classes were defined: mangroves, water bodies, bare tidal flats, and urban or built-up areas. Training and validation samples were manually and visually interpreted by integrating Global Mangrove Watch, historical mangrove datasets, and high-resolution Google Earth imagery. To ensure temporal consistency, training samples were selected from stable areas where land-cover types could be reliably identified across multiple years. The sample dataset was randomly divided into training and testing subsets using a 7:3 ratio. The RF model was configured with 20 decision trees and a bootstrap sample ratio of 0.8.

Classification accuracy was assessed using independent validation samples. Overall accuracy, producer's accuracy, user's accuracy, and the Kappa coefficient were calculated from confusion matrices. The annual mangrove classification achieved an overall accuracy greater than 90% and a Kappa coefficient greater than 0.9 (Fig. S1B), indicating that the classification results were suitable for analyzing multi-decadal mangrove dynamics at the delta scale.

Because single-date Landsat imagery is sensitive to tidal stage, mangrove seaward edges may be partially submerged during high tide, causing underestimation of mangrove extent (You et al., 2023; Zhou et al., 2024). We therefore used annual median composites to reduce tidal noise. To validate this approach, mangrove seaward edges derived from annual median composites were compared with those derived from three optimal low-tide Landsat scenes using the Digital Shoreline Analysis System, DSAS. A $\pm$ 30 m tolerance threshold, corresponding to one Landsat pixel, was used to evaluate boundary agreement. The mean boundary discrepancies ranged from -10.91 m to $+10.29$ m, and nearly 50% of the compared boundary segments showed perfect overlap (Figs. S3, S4). This result indicates that annual median composites effectively reduce tidal-induced boundary uncertainty and are appropriate for extracting long-term mangrove extent in the Mekong Delta.

The potential influence of mixed pixels associated with 30-m Landsat imagery was also evaluated. Mangroves in the Mekong Delta are generally characterized by extensive and contiguous canopies rather than narrow, highly fragmented fringing patches. Patch-size analysis for representative epochs showed that large mangrove patches greater than 1 ha, equivalent to more than 11 Landsat pixels, accounted for 89.7%, 88.1%, and 91.3% of total mangrove extent in 1995, 2008, and 2020, respectively (Table S3). Therefore, mixed-pixel uncertainty is mainly restricted to patch margins and is unlikely to substantially affect delta-scale estimates of mangrove area change (Bullock et al., 2017). Nevertheless, we acknowledge that the 30-m spatial resolution limits the detection of fine-scale ecological processes and sub-pixel degradation.

2.3. Measurements of mangrove changes

Using the spatial analysis tools in ArcGIS (Scott and Janikas, 2009), we quantified the unchanged, gained, and lost mangroves for the periods of 1992–1997, 1997–2002, 2002–2007, 2007–2012, 2012–2017, 2017–2024, and 1992–2024. Mangrove area statistics were conducted across the entire Mekong Delta and its subregions (SC, CC and NE) to characterize spatiotemporal dynamics. Mangrove seaward edges were delineated for years 1992, 1997, 2002, 2007, 2012, 2017 and 2024. The Digital Shoreline Analysis System (DSAS) generated 3811 cross-sections perpendicular to the baseline of mangrove seaward edges at 100 m intervals. For each cross-section, two key indicators were derived—the azimuth angle and the End Point Rate (EPR)—which respectively represent the spatial location and the rate of coastal erosion or deposition. The azimuth specifies the exact geographic position and directional orientation of the eroding or accreting shoreline. The End Point Rate (EPR) was used to calculate the rate of mangrove seaward edge expansion or retreat. The EPR is a linear ratio between the positional difference of the earliest and latest phases and the time span, which effectively accommodates both non-equidistant time intervals of remote sensing imagery acquisition and non-linear changes along delta fronts influenced by tidal and sedimentary dynamics (Genz et al., 2007; Thieler et al., 2009).

2.4. Statistical analysis

The dynamics of mangrove seaward and landward migration in the Mekong Delta were reflected by changes in mangrove area and seaward edges across the entire Mekong Delta and its subregions. To minimize the influence of outliers, annual time-series data for mangrove area and seaward edges were aggregated into 5-year averages. We then calculated the fluvial sediment load and relative sea level values for corresponding periods. Correlation analyses were conducted to assess the relationships between: (1) annual mean mangrove area/mangrove seaward edge change rate and annual mean fluvial sediment load and (2) annual mean mangrove area/mangrove seaward edge change rate and annual mean relative sea level during the same periods. Statistical significance was determined using *p*-values, with a less stringent threshold ($p < 0.1$) applied to account for the limited number of temporal intervals, particularly in cases with moderately strong correlation coefficients.

We did not attempt to quantitatively partition the relative contributions of sediment supply, relative sea-level rise, and anthropogenic interventions using a single attribution model, because these drivers are characterized by different spatial and temporal resolutions and are strongly interdependent. Fluvial sediment load and relative sea level are available mainly as delta-scale annual time series, whereas anthropogenic interventions such as seawalls, shrimp ponds, and restoration measures are spatially heterogeneous and lack consistent annual records for the full study period. Therefore, our analysis focuses on identifying statistical associations between mangrove dynamics and sediment and relative sea level variability, and on interpreting these associations using spatial contrasts among coastal sectors with different geomorphic settings and degrees of human constraint.

3. Results

3.1. Gains and losses of mangroves

The Mekong Delta experienced a net mangrove expansion of approximately 46300 ha, characterized by three distinct temporal phases. The most rapid growth occurred from 1992 to 2001, averaging 3146.47 ha/yr, followed by a transitional decline phase from 2001 to 2010 with a loss of −1788.20 ha/yr. Subsequently, an accelerated recovery phase began, reaching a growth rate of 2431.61 ha/yr by 2024 (Fig. 2A). Furthermore, mangrove expansion exhibited spatially heterogeneous patterns across the estuarine and coastal zones. The NE experienced an initial contraction phase from 1992 to 2003, with a loss rate of 806.32 ha/yr, before transitioning to increase at 313.77 ha/yr through 2024 (Fig. 2B). In contrast, the CC exhibited fluctuating but overall increasing mangrove area at 161.72 ha/yr (Fig. 2C). Notably, the SC dominated mangroves expansion, contributing nearly half of the total mangrove gains through sustained growth averaging 1096.96 ha/yr (Fig. 2D).

From 1992 to 2024, landward expansion dominated in the Mekong Delta, accounting for an area approximately three times greater than seaward progression (Fig. 3; Table S4). Landward losses also affected the net change, with the lowest landward reduction occurring between 2012 and 2017 (Figs. 3B, S5E), coinciding with peak overall net gains (Fig. 3A). Although seaward zones showed net increases overall, the expansion rate declined sharply after 2002 (Figs. 3C, S5C–F). This was accompanied by progressively intensifying seaward losses (Fig. 3B), potentially linked to RSLR (Osland et al., 2022; Alongi, 2008).

Mangrove gains and losses exhibited notable spatiotemporal heterogeneity (Fig. 4A). In the NE, losses and gains nearly balanced, resulting in minimal net area change (Fig. 3D). The NE incurred landward losses of 6047.95 ha in Tra Vinh and Ben Tre, while acquiring 7505.79 ha through seaward expansion between 1992 and 2024 (Table S4). Simultaneously, the CC showed modest net gains in both landward and seaward zones (Fig. 3D). The strongest changes occurred

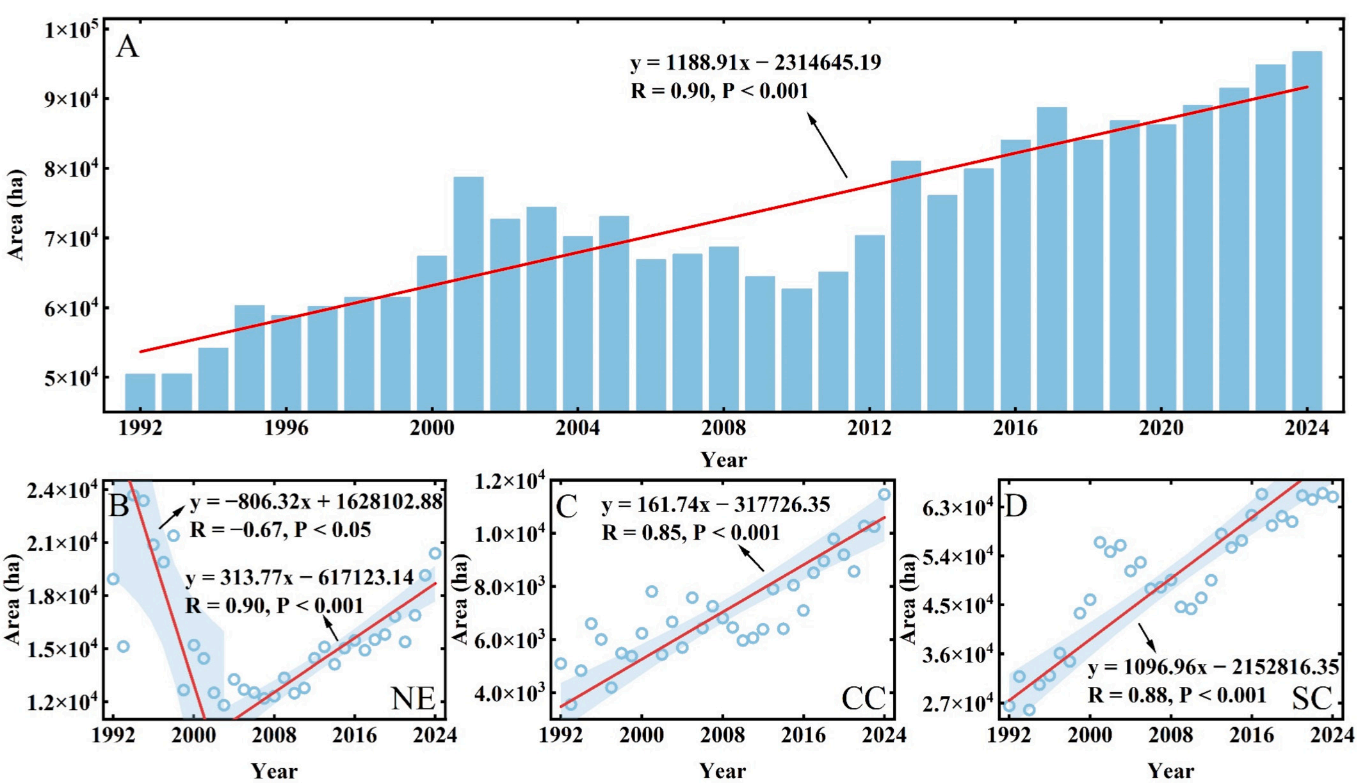

Fig. 2. Mangrove area changes in the Mekong Delta from 1992 to 2024. (A) Mekong Delta; (B) North Estuary (NE); (C) Central Coast (CC); (D) South Coast (SC).

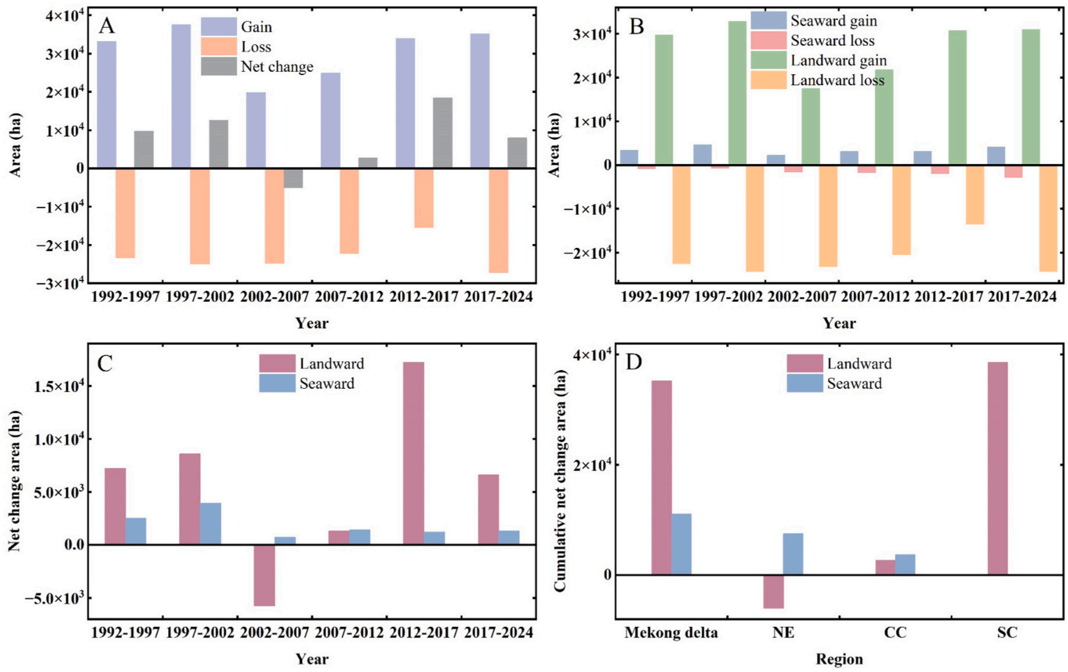

Fig. 3. Mangrove gains and losses in the Mekong Delta from 1992 to 2024. (A) Mangrove gains, losses, and net changes; (B) Mangrove gains and losses both landward and seaward; (C) Net landward and seaward mangrove changes; (D) Net mangrove changes in the NE, CC and SC.

in the SC, where landward expansion accounted for 38552.9 ha of gains, while seaward gains and losses effectively offset each other during the study period (Fig. 3D; Table S4).

3.2. Mangrove seaward edge changes

Mangrove seaward edges in the Mekong Delta expanded at an average rate of 5.99 m/yr during 1992–2024 (Fig. 4B–C). Of the total mangrove edges, 42% experienced landward retreat at an average rate of −17.47 m/yr, while 56% expanded seaward at 23.50 m/yr. Overall, the NE and CC displayed net expansion trends, whereas the SC exhibited a retreating pattern. Specifically, the NE expanded at an average rate of 10.86 m/yr, with 23% retreating at −7.66 m/yr and 74% expanding at 17.07 m/yr. Seaward expansion dominated in the west of river mouths and deltaic islands (Fig. 4 B3), whereas retreat dominated the eastern side (Fig. 4B4). The CC expanded at an average rate of 11.01 m/yr, with 34% retreating at −5.47 m/yr and 64% expanding at 20.12 m/yr. Expansion occurred along the southwestern and southeastern coast of Bac Lieu and Soc Trang (Fig. 4B). The SC exhibited the most dynamic changes, with maximum expansion rate exceeding 100 m/yr (Fig. 4 B1) and retreat rate below −50 m/yr (Fig. 4 B2).

3.3. Associations with river sediment supply and relative sea-level change

To examine the potential links between mangrove migration, river sediment supply, and relative sea-level change, we compared the multi-year average time-series trends of mangrove area, seaward edge migration rate, fluvial sediment load, and relative sea level in the Mekong Delta (Fig. S6). Statistical analyses revealed no significant correlation between fluvial sediment load and total mangrove area, but identified a positive correlation between fluvial sediment load and mangrove seaward edge change rate (Fig. 5A–B). This result suggests that interannual variations in sediment supply were more closely associated with seaward edge dynamics than with total mangrove area. The long-term decline in sediment supply may have contributed to the attenuation of seaward mangrove expansion, with slowed or locally reversed seaward progression in some sectors (Fig. S6B). In the SC, a significant positive correlation ($p < 0.05$) between fluvial sediment load and mangrove seaward edge change rate was observed (Fig. 5B), likely reflecting the dependence of tidal-flat accretion and mangrove establishment on suspended sediment availability (Balke et al., 2015; Xie et al., 2020).

A significant positive correlation emerged between relative sea level and mangrove area, whereas no significant relationship was found between relative sea level and mangrove seaward edge change rate (Fig. 5C–D). This pattern suggests that relative sea-level rise was more closely associated with landward expansion and total area change than with seaward edge migration. However, this association should not be interpreted as a direct or universally positive effect of sea-level rise on mangrove expansion. Rather, RSLR can create potential landward accommodation space, but whether this space is colonized by mangroves depends on sediment redistribution, substrate elevation, and the absence of artificial barriers.

Spatial differences among the NE, CC, and SC sectors provide additional context for interpreting these associations. In the NE, no significant correlation was found between relative sea level and mangrove area (Fig. 5C), probably because estuarine shorelines are more frequently constrained by seawalls and other human infrastructure (Nguyen et al., 2022; Veettil et al., 2019). By contrast, along many coastal tidal-flat areas of the SC and CC, fewer artificial barriers occur landward of existing mangroves, allowing greater potential for landward migration. Therefore, the contrast between constrained estuarine zones and less constrained coastal sectors provides qualitative evidence that anthropogenic barriers mediate the mangrove response to RSLR.

3.4. Spatial variations of coastal hydrodynamics

Offshore wave conditions showed clear spatial heterogeneity along the Mekong Delta coast, corresponding closely to the observed patterns of mangrove seaward edge change. Cross-sectional analyses indicated that 88% of erosion zones were exposed to dominant east-northeast waves (Figs. 6, S7). In the eastern sectors of SC, CC, and NE, east-northeast waves with significant wave heights exceeding 1 m accounted for 17%, 20%, and 22% of wave occurrences, respectively (Fig. 6B–D). These wave-exposed sectors corresponded to average mangrove seaward edge retreat rates of −27.06 m/yr, −6.81 m/yr, and

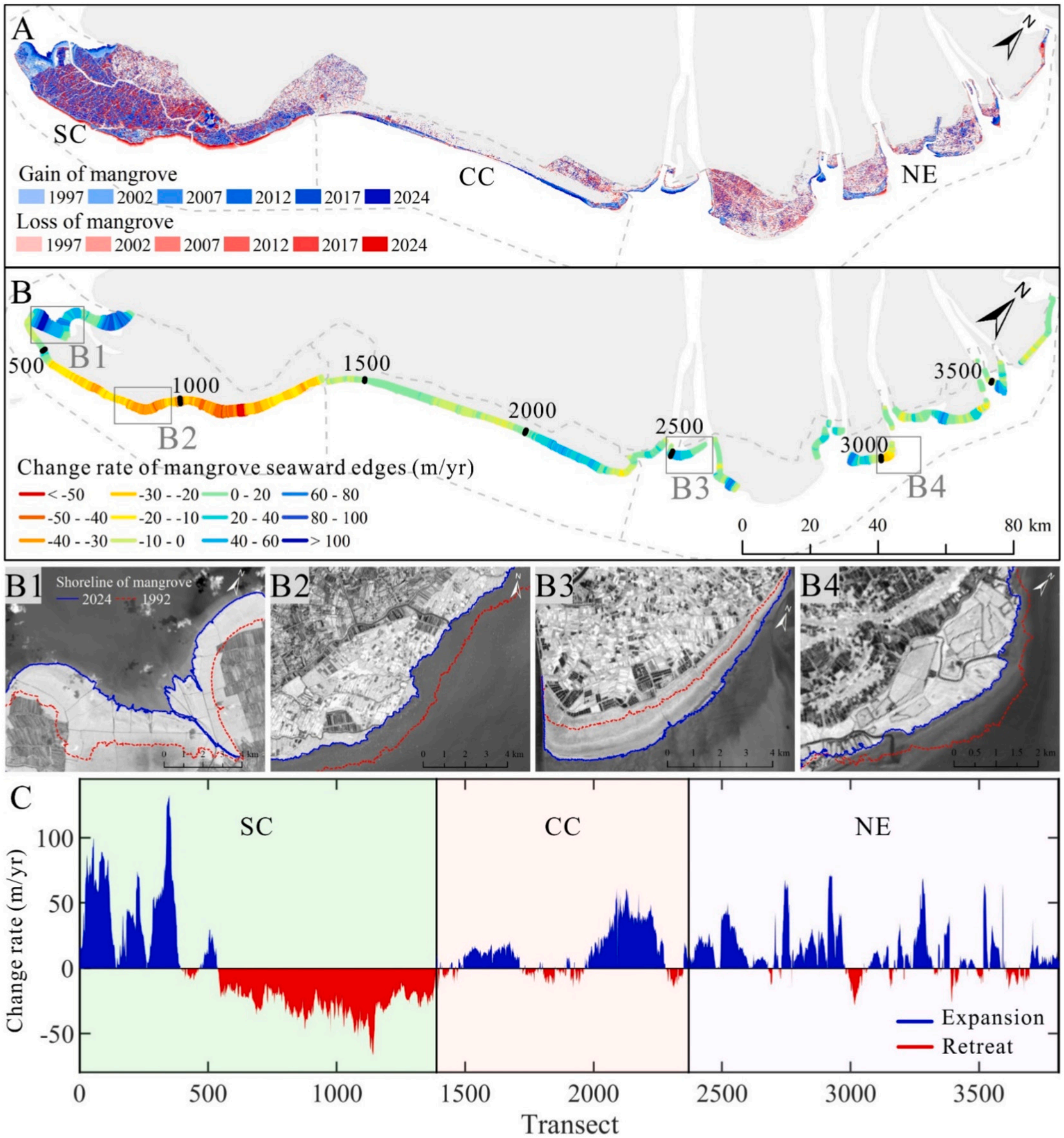

Fig. 4. Migration of mangroves in the Mekong Delta from 1992 to 2024. (A) Spatiotemporal dynamics of mangrove gains and losses; (B) Change rate of mangrove seaward edges, with numbers indicating the spatial locations of the 3811 cross-sections; (C) Expansion or retreat pattern of mangrove seaward edges in SC, CC and NE.

− 9.77 m/yr, respectively (Figs. 4, S8).

By contrast, wave-sheltered areas located west of river mouths and deltaic islands exhibited lower hydrodynamic energy and were associated with seaward mangrove expansion. These sheltered environments were particularly evident near the Song Co Chien and Cung Hau river mouths (Fig. S9). The western sector of SC was characterized by a multidirectional wave climate, with only 5% of west-southwest waves exceeding a significant wave height of 1 m (Fig. 6A). In this low-energy setting, the mangrove seaward edge expanded at an average rate of 49.64 m/yr (Figs. 4, S5). Tropical cyclones further contributed to episodic sediment redistribution along the coast. More than 80% of cyclones coincided with southwestward offshore currents (Figs. S10, S11), which likely promoted sediment transport from river mouths toward the SC sector.

4. Discussion

4.1. Local hydrodynamics modulate mangrove response to sediment reduction

Reduced fluvial sediment supply has often been regarded as a primary driver of mangrove degradation in the Mekong Delta and other large tropical deltas (Sánchez-Núñez et al., 2019; Xiong et al., 2024). However, our results indicate that the response of mangrove seaward edges cannot be explained by sediment reduction alone. Rather than quantitatively partitioning the contribution of sediment reduction, our analysis shows that seaward edge migration was statistically associated with sediment supply and that this association varied strongly among hydrodynamic settings. Mangrove dynamics are likely governed by the interaction between sediment availability, wave exposure, coastal morphology, and human modification of the shoreline. This interaction generates strong spatial heterogeneity, whereby some mangrove seaward edges retreat rapidly under energetic wave conditions, whereas others continue to expand in locally sheltered depositional environments (Long et al., 2021).

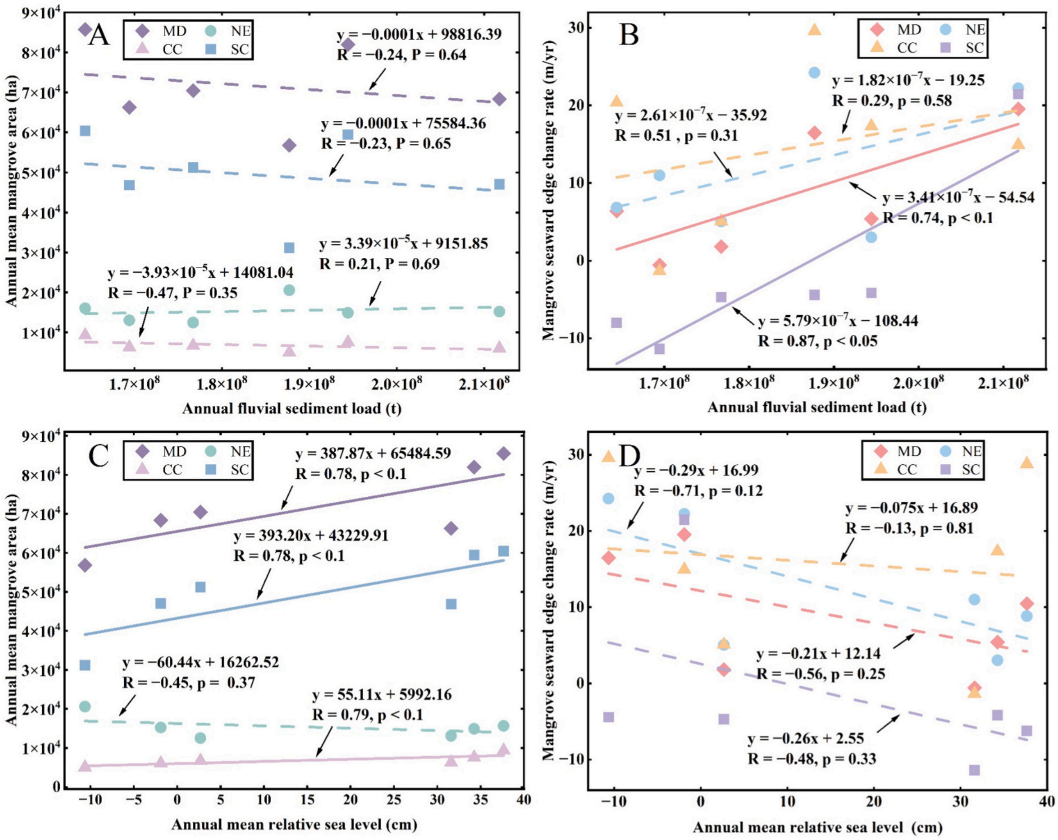

Fig. 5. Statistical associations between mangrove changes, fluvial sediment load, and mean relative sea level in the Mekong Delta. (A) Relationship between annual mean mangrove area and annual mean fluvial sediment load; (B) relationship between mangrove seaward edge change rate and annual mean fluvial sediment load; (C) relationship between annual mean mangrove area and annual mean relative sea level; (D) relationship between mangrove seaward edge change rate and annual mean relative sea level. MD: Mekong Delta; NE: North Estuary; CC: Central Coast; SC: South Coast.

The partial inconsistency between our findings and previous studies likely arises from differences in spatial scale and process representation. Earlier assessments commonly emphasized the delta-wide decline in riverine sediment delivery caused by upstream dam construction, sand mining, and channel modification (Allison et al., 2017; Li et al., 2017; Wang et al., 2011). While this perspective is essential for understanding the long-term vulnerability of the Mekong Delta, it tends to treat the coast as a relatively uniform sediment-starved system. Such a framework may overlook the fact that mangrove establishment and retreat occur at much finer spatial scales, where local hydrodynamic conditions determine whether the remaining sediment is retained, reworked, or exported offshore (Dai et al., 2024). This is particularly true when comparing estuarine and open-coast settings. In estuarine areas, distributary-channel variability can redistribute sediment unevenly among adjacent mangrove seaward edges, producing strong alongshore contrasts in accretion. In open-coast areas, however, the absence of direct fluvial focusing means that accretion depends more on local wave shelter, embayment geometry, and sediment trapping efficiency, so the response is typically more discontinuous and spatially patchy.

Our results suggest that sediment supply, while a foundational control, has its impact modulated by local hydrodynamic conditions and coastal morphology. The spatially heterogeneous response of mangroves is consistent with this interpretation. Localized wave-sheltered zones may buffer against the regional sediment deficit by reducing nearshore turbulence and promoting the trapping and deposition of fine suspended sediment. These natural refugia are often found in the lee of estuary shoals, behind deltaic islands, or within irregular coastlines. Furthermore, episodic events such as tropical cyclones may enhance sediment redistribution, potentially supporting mudflat accretion and subsequent mangrove colonization, particularly within sheltered zones (Balke et al., 2015; Xie et al., 2020; Huang and Zhu, 2023).

4.2. Resilience of mangroves to sea-level rise

Rising sea levels pose major threats to coastal wetlands (Osland et al., 2022), contributing to the loss of approximately 10–15% of global mangroves and driving landward retreat of these ecosystems (Alongi, 2008; Liang et al., 2023; Mafi-Gholami et al., 2020). Data from the My Thanh tide gauge station, situated near the mangrove seaward edge, indicate an annual mean RSLR of 23 mm/yr in the Mekong Delta (Fig. 1D). Importantly, this relative sea-level signal integrates both oceanographic sea-level rise and vertical land motion, including natural compaction and anthropogenically induced subsidence. Land subsidence may be a particularly important component of relative sea-level rise in the Mekong Delta. Previous studies have reported that some areas of the delta may experience subsidence rates of 20–25 mm/yr, largely associated with sediment compaction, groundwater extraction, and other anthropogenic activities (Minderhoud et al., 2019).

Despite these challenges, a net mangrove expansion was observed in the Mekong Delta, with three-quarters occurring landward and one-quarter seaward (Fig. 4D). This pattern should not be interpreted as evidence that sea-level rise directly causes mangrove expansion. Instead, it reflects the complex interactions among RSLR, sediment availability, accommodation space, and human constraints, which together regulate mangrove ecosystem resilience (Woodroffe et al., 2016). Mangrove seaward expansion can occur only where sediment supply and local deposition are sufficient to keep pace with RSLR and support tidal-flat accretion (Enwright et al., 2016; Lovelock et al., 2015). Similar adaptation strategies have been observed in the Pearl River estuary, the Leichhardt River estuary, and the deltas of the Nanliu, Beilun, and Red

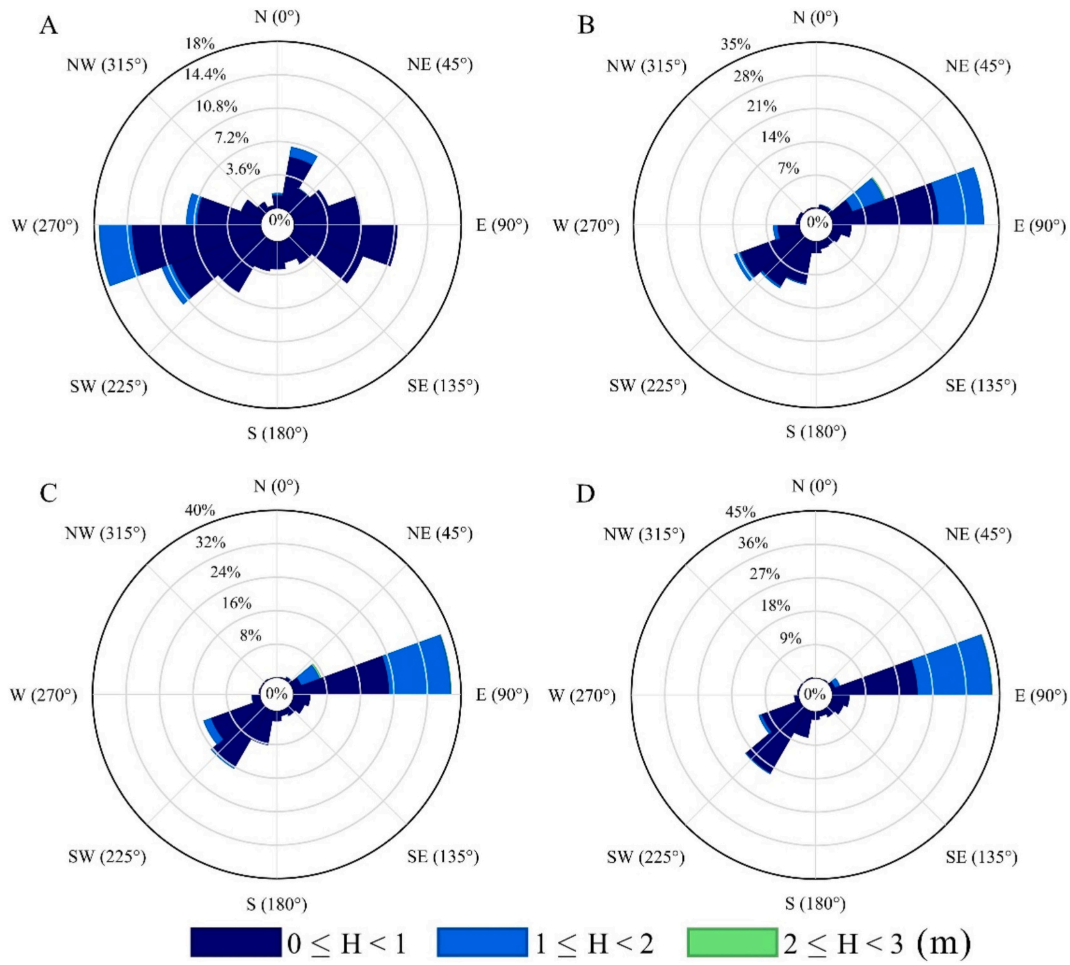

Fig. 6. Offshore wave direction and height distribution along the Mekong Delta coast. (A) West coast of the SC; (B) East coast of the SC; (C) CC; (D) NE.

Rivers (Asbridge et al., 2016; Dai et al., 2024; Feng et al., 2020).

A complementary survival mechanism is adaptive landward migration (Borchert et al., 2018; Enwright et al., 2016). The dominant landward expansion observed in the Mekong Delta is consistent with the creation and subsequent occupation of landward accommodation space. As RSLR increases water levels, it may generate new potential habitats inland; however, continuous sediment redistribution is essential to elevate the substrate and enable mangrove establishment (Rogers et al., 2019; Woodroffe et al., 2016). Importantly, this process is viable only where inland habitats remain physically accessible. Divergent migration patterns in estuarine and coastal regions underscore this constraint. In the NE, seawalls and other anthropogenic barriers restrict landward accommodation, whereas many coastal tidal-flat sectors in the SC and CC remain less constrained and therefore allow greater potential for landward migration.

4.3. Conservation policies for mangrove landward migration

The landward migration of mangroves in the Mekong Delta has been constrained by the construction of seawalls and shrimp ponds (Nguyen et al., 2022; Veettil et al., 2019). Although a full quantitative time series of anthropogenic interventions was unavailable for this study, their spatial distribution provides important qualitative evidence for interpreting the observed migration patterns. Seawalls have primarily been constructed landward of existing mangroves in the estuarine zones, whereas many open-coast sectors have fewer artificial barriers. This uneven development of the shoreline creates a contrast between constrained coastal squeeze and relatively unhindered landward migration, helping to explain why mangrove responses to RSLR differ among sectors.

Restrictions associated with seawalls are primarily concentrated in the NE, whereas constraints related to shrimp ponds are mainly found in the CC and SC. In response, the Vietnamese government implemented a series of conservation policies (Hai et al., 2020; Thuc et al., 2016). In 1991, legislation mandated that mangroves constitute at least 70% of land designated for aquaculture and agriculture (Li et al., 2020). However, these efforts have not achieved consistent success (Phan and Stive, 2022). Between 2002 and 2012, mangrove loss occurred concurrently with limited landward expansion (Figs. 3B–C, S5C–D), as human activities likely constrained migration, probably linked to the relaxation of conservation policies. Subsequent policy enhancements targeting mangrove protection and restoration (Pham et al., 2022; Tinh et al., 2022) were associated with increased landward migration (Figs. 3B–C, S5E), fostering integrated mangrove-aquaculture ecosystems (Fig. S12). Nonetheless, ongoing anthropogenic pressures continue to hinder mangrove migration, highlighting the necessity of robust regulatory enforcement. Without such measures, economic exploitation may further degrade mangrove habitats, disrupt ecological balance, exacerbate the impacts of rising sea level, and accelerate delta instability.

4.4. Limitations and broader implications

Although our study provides a comprehensive multi-decadal assessment of delta-scale mangrove dynamics, the reliance on 30-m Landsat imagery introduces inherent analytical constraints. First, the 30-m resolution limits our minimum mapping unit, making fine-scale ecological processes undetectable. Therefore, the mangroves dynamic in this study should be strictly interpreted as macro-scale trends involving aggregate areal changes of thousands of hectares. Second, sub-pixel noise can affect the overall mangrove classification. Our validation using low-tide single-date imagery confirmed that annual median composites effectively reduce tidal and atmospheric noise, keeping boundary uncertainties within one pixel (Figs. S2–S4). However, sub-pixel phenological or tidal changes may still affect the result. Future studies tracking mangrove restoration or sub-pixel degradation will require higher-resolution sensors, such as Sentinel-2 or commercial sub-meter imagery. Nonetheless, for identifying multi-decadal drivers dating back to the 1990s, the Landsat archive remains the only viable and systematic data source.

This study identifies statistical associations and spatial contrasts among mangrove dynamics, fluvial sediment supply, relative sea level, hydrodynamic exposure, and anthropogenic constraints, but it does not provide a strict quantitative partitioning of their relative contributions. Such partitioning is limited by the different spatial and temporal resolutions of the available datasets. Fluvial sediment load and relative sea level are represented mainly by delta-scale annual records, whereas mangrove changes, wave exposure, shoreline morphology, seawalls, shrimp ponds, and restoration activities vary at much finer spatial scales. Moreover, the drivers are interdependent: sediment effects are modulated by hydrodynamic exposure, and the influence of RSLR depends on sedimentation and the availability of landward accommodation space. Therefore, our interpretation focuses on likely dominant controls inferred from correlations, sectoral contrasts, and geomorphic mechanisms. Future attribution work should integrate time-resolved maps of anthropogenic infrastructure, local sediment accretion measurements, subsidence observations, and hydrodynamic modeling to more rigorously quantify the relative contributions of these interacting drivers.

From a management perspective, the findings are transferable to other deltaic mangrove systems primarily at the level of process understanding rather than as direct numerical rates. The observed Mekong Delta pattern—attenuated seaward expansion under declining fluvial sediment supply, combined with landward migration where accommodation space remains available—highlights a general management principle relevant to many sediment-starved deltas. In systems where upstream damming, sand mining, river regulation, or channel engineering have substantially reduced fluvial sediment delivery, the capacity of mangroves to expand seaward or keep pace vertically with relative sea-level rise is likely to weaken, particularly along exposed coasts with limited mudflat accretion (Woodroffe et al., 2016). Under such conditions, conservation strategies that rely only on seaward colonization or coastal afforestation may become increasingly ineffective unless sediment availability and hydrodynamic suitability are maintained or restored.

However, transferability will depend strongly on local sediment regimes, tidal range, wave climate, subsidence rate, coastal morphology, and the intensity of human pressures. In river-dominated deltas with continued sediment delivery, such as relatively sediment-rich distributary mouths, mangrove expansion may remain strongly controlled by mudflat formation and shoreline progradation (Woodroffe et al., 2016). In contrast, in dam-impacted or sediment-deficient deltas, such as parts of the Chao Phraya, Irrawaddy, or Ganges-Brahmaputra-Meghna systems, mangrove persistence may depend more heavily on landward accommodation space, sediment trapping efficiency, and the removal or redesign of hard coastal barriers (Bidorn et al., 2021; Bomer et al., 2020; Xiong et al., 2024). Therefore, the Mekong case suggests that deltaic mangrove management should move beyond static protection boundaries and adopt dynamic adaptation planning, including the protection of landward migration corridors, stricter control of coastal squeeze from aquaculture and infrastructure, sediment-sensitive river-basin management, and spatial prioritization of restoration in areas where geomorphic conditions can support long-term mangrove persistence.

5. Conclusion

The Mekong Delta experienced a net mangrove expansion of approximately 46300 ha over the past three decades, with seaward edge expansion at an average rate of 5.99 m/yr. Mangrove expansion differs between seaward and landward directions, with approximately three-quarters occurring landward and one-quarter seaward. Reduced river sediment supply has attenuated seaward mangrove expansion trends, while RSLR is a key factor in the landward zones, creating potential accommodation space that can facilitate mangrove migration into inland habitats where physical barriers are absent. The observed landward migration represents a key resilience mechanism, allowing mangroves to adapt to rising sea levels where accommodation space is available. However, deltaic mangroves are increasingly threatened by compounding pressures from rising sea level and coastal squeeze, which may precipitate potential ecosystem collapse. Thereafter, rigorous enforcement of mangrove conservation policies represents a critical priority to safeguard naturally migrating ecosystems, thereby strengthening their capacity to mitigate coastal vulnerability to rising sea levels.

CRediT authorship contribution statement

Tianliang Wu: Writing – original draft, Methodology, Formal analysis, Data curation. **Aoyang He:** Writing – original draft, Visualization, Resources, Formal analysis. **Zhijun Dai:** Writing – review & editing, Writing – original draft, Validation, Supervision, Resources, Project administration, Methodology, Investigation, Funding acquisition, Formal analysis, Conceptualization. **Xuefei Mei:** Writing – review & editing, Validation, Investigation. **Jaap H. Nienhuis:** Writing – review & editing, Validation, Resources. **Cong Mai Van:** Writing – review & editing, Resources, Investigation. **Nguyen An Binh:** Writing – review & editing, Validation, Investigation. **Sergio Fagherazzi:** Writing – review & editing, Resources, Project administration, Funding acquisition.

Declaration of competing interest

The authors declare that they have no known competing financial interests or personal relationships that could have appeared to influence the work reported in this paper.

Acknowledgements

This research was supported by National Key R&D Program of China (2023YFE0121200), and Shanghai International Science and Technology Cooperation Fund Project (24230740100). S.F. was partly funded by the USA National Science Foundation awards 2224608 (PIE LTER) and 2425178 (VCR LTER).

Appendix A. Supplementary data

Supplementary data to this article can be found online at https://doi.org/10.1016/j.ecolind.2026.115160.

Data availability

The Landsat Surface Reflectance products used for mangrove extraction are accessible via the Google Earth Engine platform (https://developers.google.com/earth-engine/datasets/catalog/landsat). Fluvial suspended sediment load data were obtained from Dethier et al. (2022) and are available on Zenodo (https://zenodo.org/records/7808492). Relative sea-level data at the My Thanh tide gauge station were provided by the Mekong River Commission, and the derived annual mean relative sea-level have been deposited in the Mendeley Data repository (doi:10.17632/cptzrxz6b6.1; https://data.mendeley.com/datasets/cptzrxz6b6/1). Hourly tide levels at Vung Tau station are acquired from the Sea Level Station Monitoring Facility at https://www.ioc-sealevelmonitoring.org/index.php. Tropical cyclones are derived from the International Best Track Archive for Climate Stewardship at https://www.ncei.noaa.gov/products/international-best-track-archive. Offshore current velocities/directions are acquired from the Copernicus Marine Service at https://data.marine.copernicus.eu/product/GLOBAL_MULTIYEAR_PHY_001_030/services. Wave heights and directions are sourced from the ECMWF ERA5 reanalysis dataset (https://cds.climate.copernicus.eu/datasets/reanalysis-era5-single-levels).

References

Allison, M.A., Nittrouer, C.A., Ogston, A.S., Mullarney, J.C., Nguyen, T.T., 2017. Sedimentation and survival of the Mekong Delta: A case study of decreased sediment supply and accelerating rates of relative sea level rise. Oceanography 30 (3), 98–109. https://doi.org/10.5670/oceanog.2017.318.

Alongi, D.M., 2008. Mangrove forests: resilience, protection from tsunamis, and responses to global climate change. Estuar. Coast. Shelf Sci. 76 (1), 1–13. https://doi.org/10.1016/j.ecss.2007.08.024.

Asbridge, E., Lucas, R., Ticehurst, C., Bunting, P., 2016. Mangrove response to environmental change in Australia's Gulf of Carpentaria. Ecol. Evol. 6 (11), 3523–3539. https://doi.org/10.1002/ece3.2140.

Balke, T., Swales, A., Lovelock, C.E., Herman, P.M., Bouma, T.J., 2015. Limits to seaward expansion of mangroves: translating physical disturbance mechanisms into seedling survival gradients. J. Exp. Mar. Biol. Ecol. 467, 16–25. https://doi.org/10.1016/j.jembe.2015.02.015.

Baloloy, A.B., Blanco, A.C., Ana, R.R.C.S., Nadaoka, K., 2020. Development and application of a new mangrove vegetation index (MVI) for rapid and accurate mangrove mapping. ISPRS J. Photogramm. Remote Sens. 166, 95–117. https://doi.org/10.1016/j.isprsjprs.2020.06.001.

Beselly, S.M., van der Wegen, M., Grueters, U., Reyns, J., Dijkstra, J., Roelvink, D., 2021. Eleven years of mangrove–mudflat dynamics on the mud volcano-induced prograding delta in East Java, Indonesia: integrating UAV and satellite imagery. Remote Sens. 13 (6), 1084. https://doi.org/10.3390/rs13061084.

Bidorn, B., Sok, K., Bidorn, K., Burnett, W.C., 2021. An analysis of the factors responsible for the shoreline retreat of the Chao Phraya Delta (Thailand). Sci. Total Environ. 769, 145253. https://doi.org/10.1016/j.scitotenv.2021.145253.

Bomer, E.J., Wilson, C.A., Hale, R.P., Hossain, A.N.M., Rahman, F.M.A., 2020. Surface elevation and sedimentation dynamics in the Ganges-Brahmaputra tidal delta plain, Bangladesh: evidence for mangrove adaptation to human-induced tidal amplification. CATENA 187, 104312. https://doi.org/10.1016/j.catena.2019.104312.

Borchert, S.M., Osland, M.J., Enwright, N.M., Griffith, K.T., 2018. Coastal wetland adaptation to sea level rise: quantifying potential for landward migration and coastal squeeze. J. Appl. Ecol. 55, 2876–2887. https://doi.org/10.1111/1365-2664.13169.

Bullock, E.L., Fagherazzi, S., Nardin, W., Vo-Luong, P., Nguyen, P., Woodcock, C.E., 2017. Temporal patterns in species zonation in a mangrove forest in the Mekong Delta, Vietnam, using a time series of Landsat imagery. Cont. Shelf Res. 147, 144–154. https://doi.org/10.1016/j.csr.2017.07.007.

Dai, Z., Long, C., Mei, X., Fagherazzi, S., Xong, Y., 2024. Overestimation of mangroves deterioration from sea level rise in tropical deltas. Geophys. Res. Lett. 51 (19). https://doi.org/10.1029/2024GL109675 e2024GL109675.

Dethier, E.N., Renshaw, C.E., Magilligan, F.J., 2022. Rapid changes to global river suspended sediment flux by humans. Science 376 (6600), 1447–1452. https://doi.org/10.1126/science.abn7980.

Donato, D.C., Kauffman, J.B., Murdiyarso, D., Kurnianto, S., Stidham, M., Kanninen, M., 2011. Mangroves among the most carbon-rich forests in the tropics. Nature Ggeoscience 4 (5), 293–297. https://doi.org/10.1038/NGEO1123.

Enwright, N.M., Griffith, K.T., Osland, M.J., 2016. Barriers to and opportunities for landward migration of coastal wetlands with sea-level rise. Front. Ecol. Environ. 14, 307–316. https://doi.org/10.1002/fee.1282.

Feng, Z., Tan, G., Xia, J., Shu, C., Chen, P., Wu, M., Wu, X., 2020. Dynamics of mangrove forests in Shenzhen Bay in response to natural and anthropogenic factors from 1988 to 2017. J. Hydrol. 591, 125271. https://doi.org/10.1016/j.jhydrol.2020.125271.

Genz, A.S., Fletcher, C.H., Dunn, R.A., Frazer, L.N., Rooney, J.J., 2007. The predictive accuracy of shoreline change rate methods and alongshore beach variation on Maui, Hawaii. J. Coast. Res. 23 (1), 87–105. https://doi.org/10.2112/05-0521.1.

Hai, N.T., Dell, B., Phuong, V.T., Harper, R.J., 2020. Towards a more robust approach for the restoration of mangroves in Vietnam. Ann. For. Sci. 77, 1–18. https://doi.org/10.1007/s13595-020-0921-0.

Huang, J., Zhu, J., 2023. Suspended sediment dynamics and influencing factors during typhoons in Hangzhou Bay, China. Anthr. Coasts 6 (1), 3. https://doi.org/10.1007/s44218-023-00019-5.

Jia, M., Wang, Z., Mao, D., Ren, C., Song, K., Zhao, C., Wang, C., Xiao, X., Wang, Y., 2023. Mapping global distribution of mangrove forests at 10-m resolution. Sci. Bull. 68 (12), 1306–1316. https://doi.org/10.1016/j.scib.2023.05.004.

Kondolf, G.M., Rubin, Z.K., Minear, J.T., 2014. Dams on the Mekong: cumulative sediment starvation. Water Resour. Res. 50 (6), 5158–5169. https://doi.org/10.1002/2013WR014651.

Leuven, J.R., Pierik, H.J., Vegt, M.V.D., Bouma, T.J., Kleinhans, M.G., 2019. Sea-level-rise-induced threats depend on the size of tide-influenced estuaries worldwide. Nat. Clim. Chang. 9 (12), 986–992. https://doi.org/10.1038/s41558-019-0608-4.

Li, X., Liu, J.P., Saito, Y., Nguyen, V.L., 2017. Recent evolution of the Mekong Delta and the impacts of dams. Earth Sci. Rev. 175, 1–17. https://doi.org/10.1016/j.earscirev.2017.10.008.

Li, X., Chen, D., Duan, Y., Ji, H., Zhang, L., Chai, Q., Hu, X., 2020. Understanding land use/land cover dynamics and impacts of human activities in the Mekong Delta over the last 40 years. Global Ecology and Conservation 22, e00991. https://doi.org/10.1016/j.gecco.2020.e00991.

Liang, S., Hu, W., Liu, J., Su, S., Chen, G., Chen, S., Xie, B., Du, J., Liu, W., Chen, B., 2023. Mapping mangrove sustainability in the face of sea level rise and land use: a case study on Leizhou peninsula, China. J. Environ. Manag. 325, 116554. https://doi.org/10.1016/j.jenvman.2022.116554.

Long, C., Dai, Z., Zhou, X., Mei, X., Van, C.M., 2021. Mapping mangrove forests in the Red River Delta, Vietnam. For. Ecol. Manag. 483, 118910. https://doi.org/10.1016/j.foreco.2020.118910.

Lovelock, C.E., Cahoon, D.R., Friess, D.A., Guntenspergen, G.R., Krauss, K.W., Reef, R., Rogers, K., Saunders, M.L., Sidik, F., Swales, A., Saintilan, N., Thuyen, L.X., Triet, T., 2015. The vulnerability of Indo-Pacific mangrove forests to sea-level rise. Nature 526 (7574), 559–563. https://doi.org/10.1038/nature15538.

Mafi-Gholami, D., Zenner, E.K., Jaafari, A., 2020. Mangrove regional feedback to sea level rise and drought intensity at the end of the 21st century. Ecol. Indic. 110, 105972. https://doi.org/10.1016/j.ecolind.2019.105972.

Minderhoud, P.S.J., Coumou, L., Erkens, G., Middelkoop, H., Stouthamer, E., 2019. Mekong delta much lower than previously assumed in sea-level rise impact assessments. Nat. Commun. 10, 3847. https://doi.org/10.1038/s41467-019-11602-1.

Nguyen, H., Trung, T.H., Phan, D.C., Anh Tran, T., Thi Hai Ly, N., Nasahara, K.N., Prishchepov, A.V., Hölzel, N., 2022. Transformation of rural landscapes in the Vietnamese Mekong Delta from 1990 to 2019: a spatio-temporal analysis. Geocarto Int. 37 (26), 13881–13903. https://doi.org/10.1080/10106049.2022.2086623.

Osland, M.J., Chivoiu, B., Enwright, N.M., Thorne, K.M., Guntenspergen, G.R., Grace, J. B., Dale, L.L., Brooks, W., Herold, N., Day, J.W., Sklar, F.H., Swarzenzki, C.M., 2022. Migration and transformation of coastal wetlands in response to rising seas. Sci. Adv. 8 (26), eabo5174. https://doi.org/10.1126/sciadv.abo5174.

Pham, T.T., Vien, N.N., Vo, Q.T., Tang, T.K.H., Nguyen, T.L., Tran, N.M.H., Nguyen, T.T. A., Nguyen, T.V.A., Nguyen, N.Q., 2022. Opportunities and challenges for mangrove restoration in the Mekong Delta: status, policies and stakeholder outlook. https://doi.org/10.17528/cifor/008610.

Phan, M.H., Stive, M.J., 2022. Managing mangroves and coastal land cover in the Mekong Delta. Ocean Coast. Manag. 219, 106013. https://doi.org/10.1016/j.ocecoaman.2021.106013.

Poortinga, A., Aekakkararungroj, A., Kityuttachai, K., Nguyen, Q., Bhandari, B., Soe Thwal, N., Priestley, H., Kim, J., Tenneson, K., Chishtie, F., Towashiraporn, P., Saah, D., 2020. Predictive analytics for identifying land cover change hotspots in the Mekong region. Remote Sens. 12 (9), 1472. https://doi.org/10.3390/rs12091472.

Rogers, K., Kelleway, J.J., Saintilan, N., Megonigal, J.P., Adams, J.B., Holmquist, J.R., Lu, M., Schile-Beers, L., Zawadzki, A., Mazumder, D., Woodroffe, C.D., 2019. Wetland carbon storage controlled by millennial-scale variation in relative sea-level rise. Nature 567, 91–95. https://doi.org/10.1038/s41586-019-0951-7.

Rouse, J.W., Haas, R.H., Schell, J.A., Deering, D.W., 1974. Monitoring vegetation systems in the great plains with ERTS proceeding. . In third earth reserves technology satellite symposium,. NASA, greenbelt. SP-351 (. vol. 30103017.

Sánchez-Núñez, D.A., Bernal, G., Mancera Pineda, J.E., 2019. The relative role of mangroves on wave erosion mitigation and sediment properties. Estuar. Coasts 42, 2124–2138. https://doi.org/10.1007/s12237-019-00628-9.

Schuerch, M., Spencer, T., Temmerman, S., Kirwan, M.L., Wolff, C., Lincke, D., McOwen, C.J., Pickering, M.D., Reef, R., Vafeidis, A.T., Hinkel, J., Nicholls, R.J., Brown, S., 2018. Future response of global coastal wetlands to sea-level rise. Nature 561, 231–234. https://doi.org/10.1038/s41586-018-0476-5.

Scott, L.M., Janikas, M.V., 2009. Spatial statistics in ArcGIS. In: Handbook of applied spatial analysis: Software tools, methods and applications. Springer Berlin Heidelberg, Berlin, Heidelberg. https://doi.org/10.1007/978-3-642-03647-7_2.

Spencer, T., Schuerch, M., Nicholls, R.J., Hinkel, J., Lincke, D., Vafeidis, A.T., Reef, R., McFadden, L., Brown, S., 2016. Global coastal wetland change under sea-level rise and related stresses: the DIVA wetland change model. Glob. Planet. Chang. 139, 15–30. https://doi.org/10.1016/j.gloplacha.2015.12.018.

Temmerman, S., Meire, P., Bouma, T.J., Herman, P.M., Ysebaert, T., De Vriend, H.J., 2013. Ecosystem-based coastal defence in the face of global change. Nature 504 (7478), 79–83. https://doi.org/10.1038/nature12859.

Thieler, E.R., Himmelstoss, E.A., Zichichi, J.L., Ergul, A., 2009. The digital shoreline analysis system (DSAS) version 4.0-an ArcGIS extension for calculating shoreline change (no. 2008–1278). US Geol. Surv. DOI:. https://doi.org/10.3133/ofr20081278.

Thuc, T., Van Thang, N., Huong, H.T.L., Van Khiem, M., Hien, N.X., Phong, D.H., 2016. Climate Change and Sea Level Rise Scenarios for Vietnam. , (Report to Vietnam Ministry of Natural Resources and Environment).

Tinh, P.H., MacKenzie, R.A., Hung, T.D., Vinh, T.V., Ha, H.T., Lam, M.H., Hanh, N.T.H., Tung, N.X., Hai, P.M., Huyen, B.T., 2022. Mangrove restoration in Vietnamese Mekong Delta during 2015–2020: achievements and challenges. Front. Mar. Sci. 9, 1043943. https://doi.org/10.3389/fmars.2022.1043943.

Veettil, B.K., Quang, N.X., Trang, N.T.T., 2019. Changes in mangrove vegetation, aquaculture and paddy cultivation in the Mekong Delta: A study from Ben Tre Province, southern Vietnam. Estuar. Coast. Shelf Sci. 226, 106273. https://doi.org/10.1016/j.ecss.2019.106273.

Wang, J.J., Lu, X.X., Kummu, M., 2011. Sediment load estimates and variations in the lower Mekong River. River Res. Appl. 27 (1), 33–46. https://doi.org/10.1002/rra.1337.

Woodroffe, C., Rogers, K., McKee, K., Lovelock, C., Mendelssohn, I., Saintilan, N., 2016. Mangrove sedimentation and response to relative sea-level rise. Annu. Rev. Mar. Sci. 8, 243–266. https://doi.org/10.1146/annurev-marine-122414-034025.

Worthington, T.A., Zu Ermgassen, P.S., Friess, D.A., Krauss, K.W., Lovelock, C.E., Thorley, J., Tingey, R., Woodroffe, C.D., Bunting, P., Cormier, N., Lagomasino, D., Lucas, R., Murray, N.J., Sutherland, W.J., Spalding, M., 2020. A global biophysical typology of mangroves and its relevance for ecosystem structure and deforestation. Sci. Rep. 10 (1), 14652. https://doi.org/10.1038/s41598-020-71194-5.

Xie, D., Schwarz, C., Brückner, M.Z., Kleinhans, M.G., Urrego, D.H., Zhou, Z., Van Maanen, B., 2020. Mangrove diversity loss under sea-level rise triggered by bio-morphodynamic feedbacks and anthropogenic pressures. Environ. Res. Lett. 15 (11), 114033. https://doi.org/10.1088/1748-9326/abc122.

Xiong, Y., Dai, Z., Long, C., Liang, X., Lou, Y., Mei, X., Nguyen, B.A., Cheng, J., 2024. Machine learning-based examination of recent mangrove forest changes in the western Irrawaddy River Delta, Southeast Asia. Catena 234, 107601. https://doi.org/10.1016/j.catena.2023.107601.

Xu, H., 2006. Modification of normalised difference water index (NDWI) to enhance open water features in remotely sensed imagery. Int. J. Remote Sens. 27 (14), 3025–3033. https://doi.org/10.1080/01431160600589179.

You, H., You, Q., Tang, X., Liu, Y., Chen, J., Wang, F., 2023. A study on spatial distribution extraction of tidal inundated mangroves based on high and low tide level images. Forests 14 (6), 1145. https://doi.org/10.3390/f14061145.

Zablan, C.D.C., Blanco, A.C., Nadaoka, K., 2023. Temporal variation of threshold segmentation-based mangrove mapping indices in Karimunjawa-Kemujan islands with Sentinel images. . In IGARSS 2023-2023 IEEE international geoscience and remote sensing symposium,. IEEE. https://doi.org/10.1109/IGARSS52108.2023.10282891.

Zha, Y., Gao, J., Ni, S., 2003. Use of normalized difference built-up index in automatically mapping urban areas from TM imagery. Int. J. Remote Sens. 24 (3), 583–594. https://doi.org/10.1080/01431160304987.

Zhou, Y., Dai, Z., Liang, X., Cheng, J., 2024. Machine learning-based monitoring of mangrove ecosystem dynamics in the Indus Delta. For. Ecol. Manag. 571, 122231. https://doi.org/10.1016/j.foreco.2024.122231.